The mechanosensitive ion channel Piezo1 is inhibited by the peptide GsMTx4

Chilman Bae, **Frederick Sachs**, and **Philip A. Gottlieb**
Center for Single Molecule Biophysics, Department of Physiology and Biophysics, 301 Cary Hall, State University of New York, Buffalo, NY 14214, philgott@buffalo.edu, Phone: 716-829-5160; Fax 716-829-2569

Abstract

Cells can respond to mechanical stress by gating mechanosensitive ion channels (MSCs). The cloning of Piezo1, a eukaryotic cation-selective MSC, defines a new system to study mechanical transduction at the cellular level. Since Piezo1 has electrophysiological properties similar to endogenous cationic MSCs that are selectively inhibited by the peptide GsMTx4, we tested and found that the peptide targets Piezo1 activity. Extracellular GsMTx4 at μM concentrations reversibly inhibited ~80% of the mechanically induced current of outside-out patches from transfected HEK293 cells. The inhibition was voltage insensitive and, as seen with endogenous MSCs, the mirror image D enantiomer inhibited similarly to the L. The rate constants for binding and unbinding based on Piezo1 current kinetics provided association and dissociation rates of 7.0×10^5 $M^{-1}s^{-1}$ and $0.11 s^{-1}$ respectively and a K_D of ~ 155nM, similar to values previously reported for endogenous MSCs. Consistent with predicted gating modifier behavior, GsMTx4 produced a ~30mmHg rightward shift in the pressure-gating curve and was active on closed channels. In contrast, streptomycin, a nonspecific inhibitor of cationic MSCs, showed the use-dependent inhibition characteristic of open channel block. The peptide did not block currents of the mechanical channel TREK-1 on outside out patches. Whole cell Piezo1 currents were also reversibly inhibited by GsMTx4, and although the off-rate was nearly identical to outside out patches, differences were observed for the on-rate. The ability of GsMTx4 to target the mechanosensitivity of Piezo1 supports the use of this channel in a high throughput screens for pharmacological agents and diagnostic assays.

Piezo1 is a mechanosensitive channel (MSC) whose gene was isolated from the neuroblastoma cell line Neuro2A (1) and its electrophysiological properties are similar to many endogenous cationic mechanosensitive currents (2, 3). The unitary conductance of Piezo1 is ~25 pS with a reversal potential near 0 mV, clearly showing that mechanosensitivity is uncorrelated with ion selectivity since the cloned Trek-1 is K^+ selective (4-6). The Piezo1 (aka Fam38a) was first observed as a cellular response to the presence of senile plaque-associated astrocytes (7). The gene product accumulated at the endoplasmic reticulum (8) but has later been found at the plasma membrane (1).

A classic approach to the study of channels is the use of inhibitors. Currently, the peptide GsMTx4 is the only known inhibitor that specifically targets cation MSCs (9, 10). The peptide was originally isolated from the venom of a tarantula based on its ability to inhibit the mechanical response of channels in astrocytes (3). The 3-dimensional structure was solved by NMR and it belongs to the super-family of ICK (inhibitory cysteine knot) peptides

(11). Inhibition occurs as a gating modifier that biases the channel to the closed state, and appears to reside at the protein-membrane interface (12).

In this work we asked whether GsMTx4 can inhibit Piezo1 and showed that GsMTx4 blocked mechanosensitive currents from outside–out patches of HEK293 cells transfected with Piezo1. Peptide activity is voltage insensitive and the enantiomeric form of the peptide was equally effective in Piezo1 channel block. We also show that, GsMTx4 functions at the whole cell level, inhibiting Piezo1 whole cell currents expressed in HEK293 cells.

Experimental Procedures

Outside-out patches from Piezo1 transfected cells were recorded with an extracellular solution of 145 NaCl, 5 KCl, 3 $MgCl_2$, 10 HEPES, 0.1 $CaCl_2$, (in mM, pH adjusted to 7.3 with NaOH) and an internal solution of 133 CsCl, 10 HEPES, 5 EGTA, 3 $MgCl_2$. For studies with TREK-1, CsCl was replaced with KCl. GsMTx4 and its enantiomeric form were synthesized, folded and purified as previously described(3, 13).The mechanical stimulus was applied with a high speed pressure clamp (HSFC-1, ALA Scientific Instruments) controlled by QuBIO software (www.qub.buffalo.edu). HEK293 cells were tested 24 -48 h after transfection with FuGENE (Roche Diagnostic) using 250 ng of plasmid (Gift of A. Patapoutian, Scripps Institute). GsMTx4 was applied by an ALA perfusion system controlled by QuBIO (maximum concentration was achieved within ~7 ms (3)). All experiments were done at room temperature. Currents were sampled at 10 kHz and filtered at 2 kHz and collected using QuBIO.

Whole-cell and patch-clamp experiments were performed using an Axopatch 200B amplifier (Axon Instruments). Patch pipettes had resistance of 2–5 MΩ when filled with a solution of 133 CsCl, 10 HEPES, 5 EGTA, 1 $CaCl_2$, 1 $MgCl_2$ (in mM, pH adjusted to 7.3 with CsOH. The extracellular solution is identical to the one used above.

Whole cell mechanical stimulation utilized using a fire-polished glass pipette (tip diameter 2-4 μm) positioned at an angle of 45° to the cell. A computer-controlled-micromanipulator (MP-285, Sutter Instruments Co.) using LabVIEW software provided coarse positioning of the probe ~28 μm from the cell. From that position, a further rapid downward movement was driven by a piezoelectric stage (P-280.20 XYZ NanoPositioners, Physik Instrumente). The "threshold" is defined as depth at which the probe visibly deformed the cell. The probe velocity was 0.56 μm/ms during the upward and downward movement and the stimulus was maintained constant for 400 ms. Stimulation was applied every 6 s with a randomized series of 10 different amplitude steps that ranged in from +3 μm above and -1 μm below the threshold and applied for 2 s (Randomization minimized any effects of long term adaptation). Currents were recorded at a holding potential of -60 mV.

Results

Outside-out patches (O-O) from Piezo1 transfected HEK293 cells generated rapid transient currents in response to square pulses of pressure produced by a high speed pressure clamp (14) (Figure 1,2). The inactivation rate was voltage dependent (slowing with depolarization) and of similar magnitude and voltage dependency to that previously reported for Piezo1 (1) (Figure 1A, **controls**). Figure 1A shows the effect on mean currents (5-10 pulses) at depolarized (right) and hyperpolarized (left) potentials with pressure steps ~ 500 ms in duration spaced 2-4s apart. Inhibition (red trace) was more pronounced at hyperpolarized potentials than with depolarized, but currents returned at all potentials with washout of the peptide (blue trace). GsMTx4 applied to the intracellular face of inside-out patches produced

no inhibition (Figure S1 B, n=5), indicating that the peptide works on the extracellular side of the membrane.

A unique characteristic of GsMTx4 activity is its lack of stereochemical specificity: the mirror image D-enantiomer (D-GsMTx4) is as effective as the L supporting a long range mode of action (12). Figure 1B shows the effect of D-GsMTx4 (2.5 μM) on currents from O-O patches under conditions similar to those used for the L enantiomer (Figure 1A**, right**). The inhibition of peak currents for the D form was 29 ± 9% (n=5) and the L form, 20 ± 5 % (n=5, Figure 1C).

Next we characterized the response of the channels as a function of various pressures, in the presence and absence of L-GsMTx4, 1 - 4 μM (3, 12, 15) (Figure 2A, B). Figure 2A shows the response of an outside-out patch with increasing positive pressure and the peak current gating curve (Figure 2C **control**). A fit of those data to the Boltzmann equation yielded a half activation pressure $P_{1/2}$ = 48.7 ± 2.6 mmHg and a slope sensitivity of 6.6 ± 2.2 mmHg/ e-fold (Figure 2C). The activation pressure is somewhat higher than observed for cell-attached patches (1) probably as a result of changes in patch mechanics with excision (15). In the presence of GsMTx4 (Figure 2B), there is a rightward shift consistent with the effect of a gating modifier (12). In the presence of GsMTx4 (Figure 2B) we could not reach saturation before lysis of the patch, but if we assume that the saturation current is the same as that prior to applying GsMTx4, the fit shows $P_{1/2}$ shifted to 76.9 ± 2.2 mmHg and the slope sensitivity unchanged at 7.7± 2.5 mmHg/e-fold (Figure 2C). To test whether GsMTx4 might inhibit currents by decreasing the open channel conductance, we measured single channel current amplitudes using QuB (www.qub.buffalo.edu) and found no sensitivity to applied pressure or GsMTx4 (Figure S3 B).

We determined the binding kinetics using drug perfusion of O-O patches with channels activated by a steady pressure and at depolarized potentials to minimize inactivation (40mmHg). A concentration step of L-GsMTx4 (2.5 μM, rise time ~ 100 ms) inhibited channel activity (Figure 3). By fitting the current to a two-state model (open and inhibited) we extracted a mean association time τ_a = 0.7 ± 0.18 s (, n=5) and a mean dissociation time

τ_d = 9.4 ± 0.42 s (n=4). For the dissociation rate constant, $k_d = \frac{1}{\tau_d}$ and for association

$k_a = \frac{1}{\tau_a} - k_d$ yielding k_d = 0.11 s^{-1} and k_a =7.0 × 10^5 M^{-1}s^{-1}. The calculated equilibrium constant is K_D = 157 nM, consistent with the work of Suchyna *et al*. with astrocytes (3) and Bode *et al*. on atrial fibrillation (16).

While GsMTx4 inhibited the pressure evoked current, GsMTx4 also reversibly decreased both the mean and the variance of the resting current in resting patches. This is consistent with the presence of spontaneous background channel activity (Figure 3) resulting from tension caused by adhesion of the patch membrane to the pipette (17, 18).

As controls for transfection, we tested patches from cells transfected with genes coding either GFP (n=5) or TRPC6 (n=3) and found no mechanically activated currents in the same range of pressures (data not shown). Outside-out patches from control cells show a slowly activating mechanically induced current at high pressures that do not inactivate (Figure S3 A), but these currents are clearly distinguishable from Piezo1. To provide additional data on the specificity of GsMTx4 Piezo1, we tested extracellular GsMTx4, both D and L forms, on O-O patches of cells transfected with the K$^+$ selective MSC, TREK-1 (Figure 1S A). While we observed large mechanosensitive currents, we found no inhibition by GsMTx4. GsMTx4 is known to act on cationic MSCs as a gating modifier, pre-stressing the channel toward closed states (12). We compared the mechanisms of inhibition of the nonspecific antagonist

streptomycin (1, 19) and GsMTx4. GsMTx4 acts primarily on the closed channel since applying GsMTx4 prior to mechanical stimulation we had nearly 100% inhibition (Figure S2 A). In contrast, streptomycin acted as an open channel blocker (Figure S2 B). Application of 1 mM streptomycin for 90 seconds to resting patches inhibited subsequent channel activation but only in a use dependent fashion. We modeled the kinetics of streptomycin inhibition using a 3 state model in the MAC algorithm of QuB (20) as described in Figure S2 B.

GsMTx4 inhibited whole cell mechanosensitive responses generated by compressing a small region of the cell with a fire polished pipette held in a piezoelectric manipulator (1). Figure 4A shows the average peak response (5-10 pulses, 500ms duration) using a constant displacement (black). The magnitude of the currents increased with indentation depth (Figure 4C), but quantitation of the sensitivity is difficult since the local stress/strain varies with distance from the probe (21). L-GsMTx4 (4.0 μM, 1μm insertion depth) reversibly inhibited currents by 58 $\pm$6% (Figure 4A and 4B). As observed with patches, the D-form was as effective as L (Figure 3B). GsMTx4 shifted the gating curve rightward (to higher pressure) consistent with its action as a gating modifier. Unfortunately, in this case we cannot reliably fit the pressure-response data to a Boltzmann relationship since the local stress is not constant. A critical observation from the whole cell currents is the holding current that at rest was unchanged by GsMTx4, showing that Piezo1 is not active in resting cells.

The dissociation rate for whole cell currents was similar to that seen for O-O patches (10.0 $\pm$ 1.7 s, n=3, Figure 4D), but the association rate appeared significantly slower (see Figure 4E, 9.6 $\pm$ 3.9 s, n=10, as opposed to 0.7 s for O-O patches). This is not explained by mixing exchange time; the same perfusion system conducted the washout that was on the normal time scale, the GsMTx4 inhibition started without a latency (n=10). Direct tests of the perfusion system showed the exchange time to be on the order of 100ms. The discrepancy between whole cell and patch kinetics probably arises from the changes in cortical membrane structure that accompanies patch formation, a behavior reminiscent of the effects observed for K$^+$ channel inhibitors (22).

Discussion

We have shown that GsMTx4 targets the eukaryotic cationic MSCs Piezo1. The mechanical responses of Piezo1 channels in the patch are similar to those observed for whole cell recordings (1), including the voltage dependency of inactivation. Inhibition by GsMTx4 is relatively voltage insensitive, works at a calculated equilibrium constant previously observed for endogenous channels, and both enantiomeric forms are equally functional (3, 12).

GsMTx4 appears to be a gating modifier for Piezo1, as we could overcome its inhibition with increased pressure, and the resulting kinetics displayed comparable slope sensitivity (24). GsMTx4 shifts in $P_{1/2}$ reflect a local prestress favoring the closed state. Stabilizing the closed state appears to be the dominant effect on the channel since the presence of GsMTx4 prior to a pressure pulse inhibits Piezo1. However, we cannot exclude binding to other states (open or inactivated). All patches have a resting tension that allows access to the open state in the absence of an applied stimulus, although Figure 3 indicates that channel open probability from resting tension is small relative to the response with applied pressure. GsMTx4 has been shown to stabilize the open state for MscS inside out patches generated from giant spheroplasts (23). Nonetheless, this inhibitory mechanism is distinguishable from streptomycin, an open channel blocker that associated with use dependent inhibition (19).

The inhibitory action of GsMTx4 is specific for the extracellular face of cationic MSCs since internal application of GsMTx4 to inside-out patches of Piezo1 did not inhibit channel activity. Moreover, the K selective TREK-1 channel was not inhibited by the peptide. The asymmetry of GsMTx4's effect suggests that gating structures of Piezo1 are on the extracellular side. At the concentrations of peptide that we used, GsMTx4 is selective for cationic MSCs over other types of channels (31). This is supported by the fact that the holding current of resting cells was insensitive to GsMTx4.

We observed that the association rate was significantly slower in the whole cell recording compared to the patch. The origin of this difference is not clear but we know that the properties of membranes in patches and cells are different. Patch membranes are always under substantial tension (17, 25) while the membranes of resting cells are essentially tension free (26). We have shown that GsMTx4 does not affect resting whole cell currents, indicating that these MSCs are not active at rest compared to the patch where there is activity due to background stress.

Membranes that are under tension have a larger free volume and that will favor increased partitioning of amphipaths (27) and we know that GsMTx4 binds well to lipid bilayers (28, 29). The association kinetics may have two distinct kinetics steps: partitioning from solution into the membrane (a slow phase) and diffusion of partitioned GsMTx4 to the channels. Tension will accelerate the first step because partitioning amphipaths into the membrane requires disruption of the local phospholipid lattice to make space. If the membrane is under tension T, and the molecule occupies area A, the energy for insertion will contain the free energy term $\Delta G=TA$ (24) hence partitioning from water to the membrane is expected to be exponential in tension (30). One might expect that the dissociation rate would have a similar tension dependence, but that component may not be rate limiting.

The physiological functions of Piezo1 are postulated to involve mechanical transduction such as the sense of touch or blood pressure regulation. We previously showed that GsMTx4 inhibits both the whole cell regulatory volume decrease and MSC currents in O-O patches of NRK-49 cells (15), suggesting that Piezo1 may also serve as a sensor for cell swelling. We recently isolated the Piezo1 gene from NRK cells that is homologous to Piezo1, supporting this connection. GsMTx4 creates the tool necessary to explore the physiological role of these channels and can serve as the positive control for high throughput screens for small molecule pharmacology.

Supplementary Material

Refer to Web version on PubMed Central for supplementary material.

Acknowledgments

References

1. Coste B, Mathur J, Schmidt M, Earley TJ, Ranade S, Petrus MJ, Dubin AE, Patapoutian A. Piezo1 and Piezo2 are essential components of distinct mechanically activated cation channels. Science. 2010; 330:55–60. [PubMed: 20813920]

2. Guharay F, Sachs F. Stretch-activated single ion channel currents in tissue-cultured embryonic chick skeletal muscle. J Physio (London). 1984; 352:685–701.

3. Suchyna TM, Johnson JH, Hamer K, Leykam JF, Gage DA, Clemo HF, Baumgarten CM, Sachs F. Identification of a peptide toxin from Grammostola spatulata spider venom that blocks cation-selective stretch-activated channels. J Gen Physiol. 2000; 115:583–598. [PubMed: 10779316]

4. Patel A, Honore E. The TREK two P domain K+ channels. J Physiol. 2002; 539:647. [PubMed: 11897836]

5. Franks NP, Honore E. The TREK K2P channels and their role in general anaesthesia and neuroprotection. Trends in Pharmacological Sciences. 2004; 25:601–608. [PubMed: 15491783]

6. Dedman A, Sharif-Naeini R, Folgering JH, Duprat F, Patel A, Honore E. The mechano-gated K(2P) channel TREK-1. Eur Biophys J. 2009; 38:293–303. [PubMed: 18369610]

7. Satoh K, Hata M, Takahara S, Tsuzaki H, Yokota H, Akatsu H, Yamamoto T, Kosaka K, Yamada T. A novel membrane protein, encoded by the gene covering KIAA0233, is transcriptionally induced in senile plaque-associated astrocytes. Brain Res. 2006; 1108:19–27. [PubMed: 16854388]

8. McHugh BJ, Buttery R, Lad Y, Banks S, Haslett C, Sethi T. Integrin activation by Fam38A uses a novel mechanism of R-Ras targeting to the endoplasmic reticulum. J Cell Science. 2010; 123:51–61. [PubMed: 20016066]

9. Gottlieb, P.; Suchyna, T.; Sachs, F. Properties and Mechanism of the Mechanosensitive Ion Channel Inhibitor GsMTx4, a Therapeutic Peptide Derived from Tarantula Venom. In: Hamill, O., editor. Current Topics in Membranes and Transport. Academic Press; New York: 2006. p. 81-109.

10. Bowman CL, Gottlieb PA, Suchyna TM, Murphy YK, Sachs F. Mechanosensitive ion channels and the peptide inhibitor GsMTx-4: history, properties, mechanisms and pharmacology. Toxicon. 2007; 49:249–270. [PubMed: 17157345]

11. Oswald RE, Suchyna TM, McFeeters R, Gottlieb P, Sachs F. Solution structure of peptide toxins that block mechanosensitive ion channels. J Biol Chem. 2002; 277:34443–34450. [PubMed: 12082099]

12. Suchyna TM, Tape SE, Koeppe RE 2nd, Andersen OS, Sachs F, Gottlieb PA. Bilayer-dependent inhibition of mechanosensitive channels by neuroactive peptide enantiomers. Nature. 2004; 430:235–240. [PubMed: 15241420]

13. Ostrow KL, Mammoser A, Suchyna T, Sachs F, Oswald R, Kubo S, Chino N, Gottlieb PA. cDNA sequence and in vitro folding of GsMTx4, a specific peptide inhibitor of mechanosensitive channels. Toxicon. 2003; 42:263–274. [PubMed: 14559077]

14. Besch SR, Suchyna T, Sachs F. High-speed pressure clamp. Pflugers Arch. 2002; 445:161–166. [PubMed: 12397401]

15. Hua SZ, Gottlieb PA, Heo J, Sachs F. A mechanosensitive ion channel regulating cell volume. Am J Physiol Cell Physiol. 2010; 298:C1424–1430. [PubMed: 20457830]

16. Bode F, Sachs F, Franz MR. Tarantula Peptide Inhibits Atrial Fibrillation During Stretch. Nature. 2001; 409:35–36. [PubMed: 11343101]

17. Suchyna TM, Markin VS, Sachs F. Biophysics and structure of the patch and the gigaseal. Biophys J. 2009; 97:738–747. [PubMed: 19651032]

18. Honore E, Patel AJ, Chemin J, Suchyna T, Sachs F. Desensitization of mechano-gated K2P channels. Proc Natl Acad Sci U S A. 2006; 103:6859–6864. [PubMed: 16636285]

19. Hamill OP, McBride DW Jr. The pharmacology of mechanogated membrane ion channels. Pharmacol Rev. 1996; 48:231–252. [PubMed: 8804105]

20. Milescu LS, Akk G, Sachs F. Maximum likelihood estimation of ion channel kinetics from macroscopic currents. Biophys J. 2005; 88:2494–2515. [PubMed: 15681642]

21. Johnson, KL. Contact mechanics. Cambridge University Press; Cambridge Cambridgeshire; New York: 1985.

22. Schmidt D, Cross SR, MacKinnon R. A gating model for the archeal voltage-dependent K(+) channel KvAP in DPhPC and POPE:POPG decane lipid bilayers. J Mol Biol. 2009; 390:902–912. [PubMed: 19481093]

23. Kamaraju K, Gottlieb PA, Sachs F, Sukharev S. Effects of GsMTx4 on bacterial mechanosensitive channels in inside-out patches from giant spheroplasts. Biophys J. 2010; 99:2870–2878. [PubMed: 21044584]

24. Markin VS, Sachs F. Thermodynamics of mechanosensitivity. Phys Biol 2005/10/06. 2004:110–124.

25. Suchyna TM, Sachs F. Mechanosensitive channel properties and membrane mechanics in mouse dystrophic myotubes. J Physiol. 2007; 581:369–387. [PubMed: 17255168]

26. Dai J, Sheetz MP, Wan X, Morris CE. Membrane tension in swelling and shrinking molluscan neurons. J Neurosci. 1998; 18:6681–6692. [PubMed: 9712640]

27. Markin VS, Martinac B. Mechanosensitive ion channels as reporters of bilayer expansion. A theoretical model. Biophys J. 1991; 60:1120–1127. [PubMed: 1722115]

28. Posokhov YO, Gottlieb PA, Morales MJ, Sachs F, Ladokhin AS. Is lipid bilayer binding a common property of inhibitor cysteine knot ion-channel blockers? Biophys J. 2007; 93:L20–22. [PubMed: 17573432]

29. Posokhov YO, Gottlieb PA, Ladokhin AS. Quenching-enhanced fluorescence titration protocol for accurate determination of free energy of membrane binding. Anal Biochem. 2007; 362:290–292. [PubMed: 17184723]

30. Zheleva D, Sharma J, Panico M, Morris HR, Barber J. Isolation and characterization of monomeric and dimeric CP47-reaction center photosystem II complexes. The J Biol Chem. 1998; 273:16122–16127.

31. Redaelli E, Cassulini RR, Silva DF, Clement H, Schiavon E, Zamudio FZ, Odell G, Arcangeli A, Clare JJ, Alagon A, de la Vega RC, Possani LD, Wanke E. Target promiscuity and heterogeneous effects of tarantula venom peptides affecting Na+ and K+ ion channels. J Biol Chem. 2010; 285:4130–4142. [PubMed: 19955179]

Abbreviations

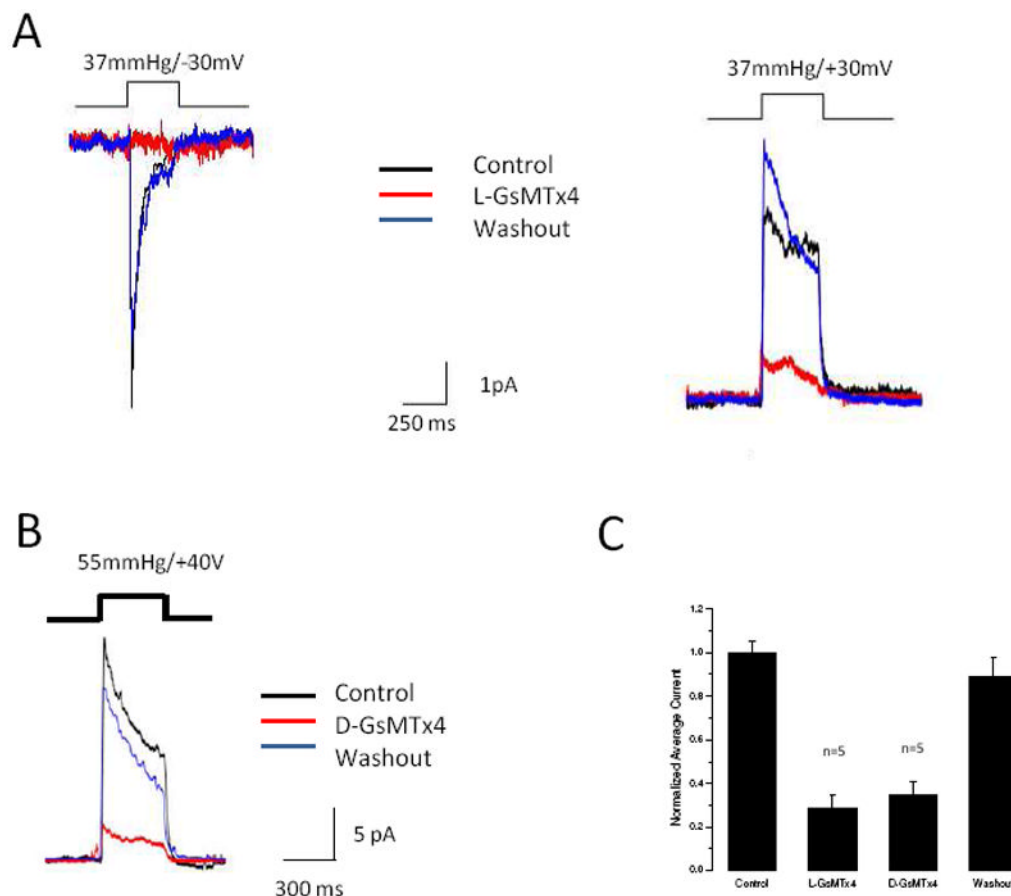|	
MSCs	mechanosensitive ion channels
GFP	green fluorescent protein
NMR	nuclear magnetic resonance
ICK	inhibitory cysteine knot

Figure 1.
GsMTx4 inhibits Piezo1 currents. **Panel A** (Left): O-O patch with the baseline response
measured at -30 mV with pressure pulses of 500 ms at intervals of 3.5 s (black trace). The
mechanical response was inhibited by L-GsMTx4 (2.5 μM, red trace) and washout restored
control activity (blue trace). The data are an average of 5-10 pulses. **Panel A (Right):** A
comparison of the -30mV response to the +30mV response shows a mild voltage
dependence of inhibition. **Panel B** demonstrates that the D-enantiomer (3.0 μM) reversibly
inhibits Piezo1. **Panel C** is a summary of the average responses to D (n=3 patches) and L
(n=7 patches) enantiomers. Data are normalized to allow comparison between experiments
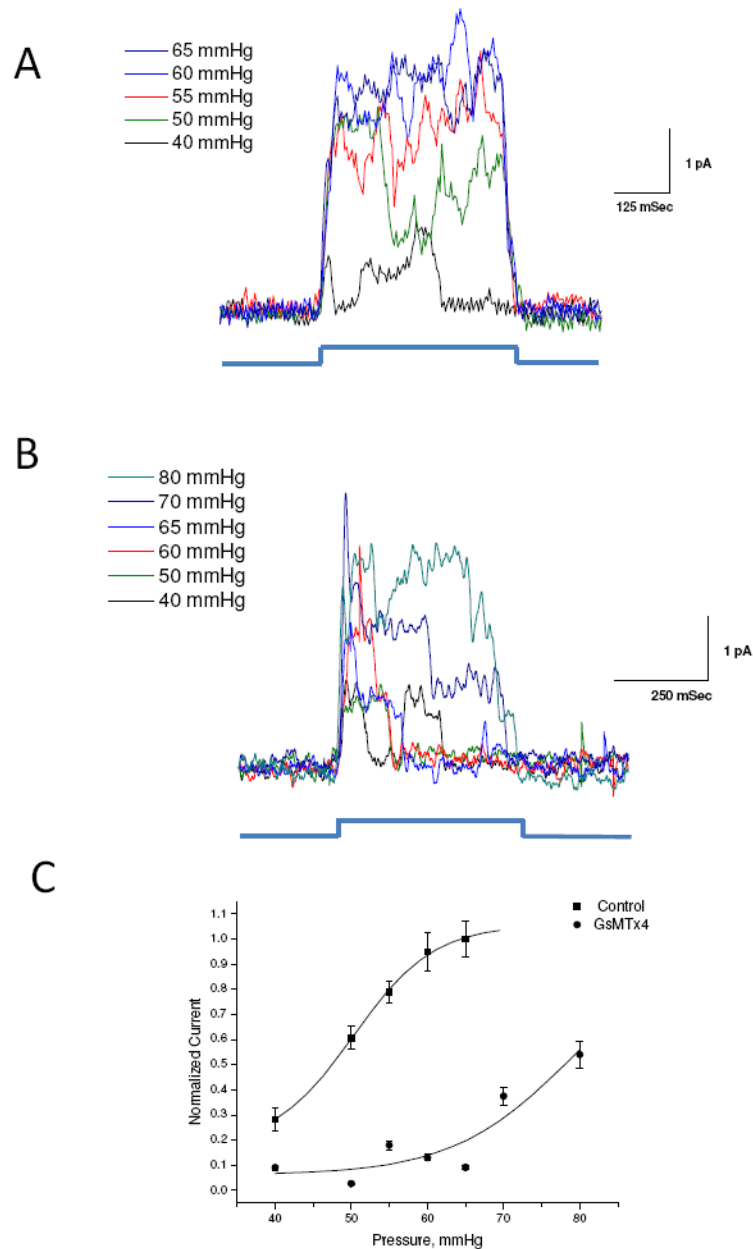and the error bars are SEM.

Figure 2.
GsMTx4 is a gating inhibitor. O-O patches were stimulated at indicated positive pressure pulses at +50 mV in the absence (**Panel A**) and in the presence of GsMTx4 (3.0 μM, **Panel B**). **Panel C** is a plot of the average peak current fit to a Boltzmann equation (black trace). In the absence of GsMTx4, the midpoint of the gating curve was 48.7 ±1.3 mmHg (SD). In the presence of GsMTx4 $P_{1/2}$= 76.8 ±2.2 mmHg (SD) (assuming a saturation current equal to that of the control).
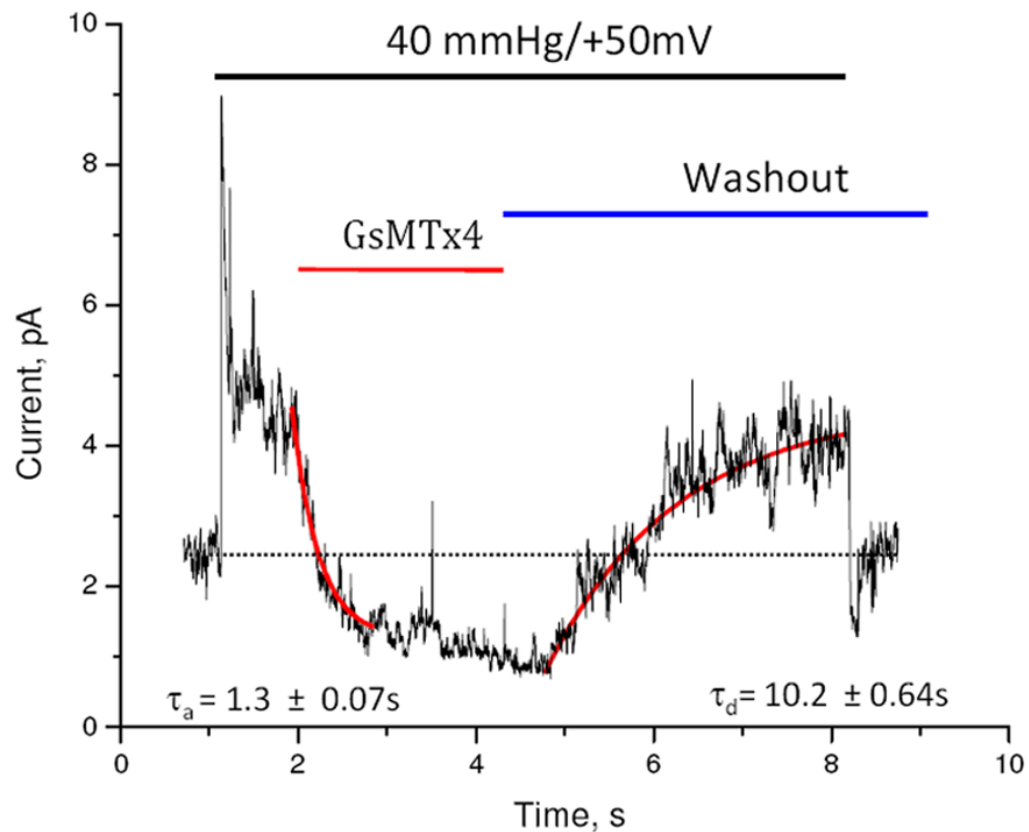
Figure 3.
Equilibrium binding constant was determined by association and dissociation kinetics. The indicated pressure pulse was applied to an outside out patch for the lifetime of the experiment. After achieving steady state, a pulse of L-GsMTx4 (2.5 μM) was perfused and inhibition reflected primarily the association rate. Washout of the peptide restored channel activity, reflecting the peptide's dissociation. Assuming the binding reaction was two states (open-blocked), we extracted the rate constants for association and dissociation from the time constants for wash-in and wash-out using the curve fitting program of QuB (curve fit shown in red, rate constants are indicated with SD). The stippled line is the baseline. GsMTx4 inhibited currents below the baseline indicating that in the "resting patch", the channels are active, probably as a result of the adhesion energy of the membrane to the glass in the seal. Note that upon the release of the pressure pulse, there is an under shoot of current caused by a transient wrinkling of the membrane. The bowed membrane under pressure has more area than membrane at equilibrium (flat disk). The wrinkled membrane has little tension and that turns off the channels. Over ~1s the membrane reanneals to the glass and restores the resting tension (see reference (18) for a full description of this effect).
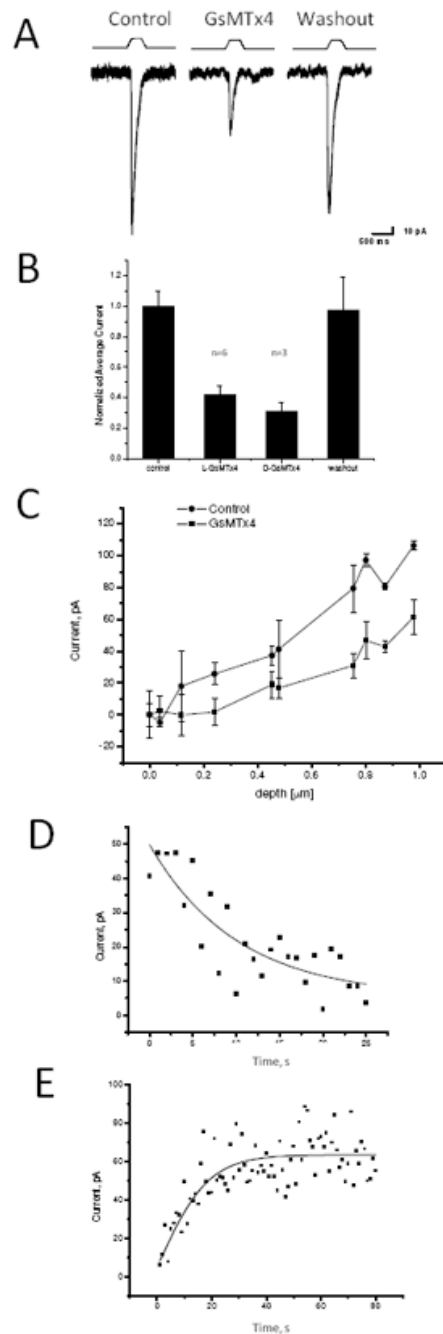
Figure 4.
Whole cell currents inhibited by GsMTx4. The cells were indented using the protocol indicated in **Panel A**. L-GsMTx4 (4.0 μM, red trace) inhibited the mechanosensitive currents (compare to the black trace), and washout returned currents to the original level (**Panel A**, blue). Notice that GsMTx4 had no effect on the holding current showing that the channels are not active in the resting cell. **Panel B**, L-GsMTx4 (4.0 μM) inhibited the mechanosensitive currents by 58 ±6% (n=6, S.D.) and the D-GsMTx4 (3.0 μM) inhibited by 70±6% (n=3 S.D.). **Panel C** demonstrates that whole cell currents increased monotonically with the depth of indentation. **Panel D** shows the mean dissociation time $\tau_d = 10.0 \pm 1.7$ s (S.D., n=3) was estimated by fitting the recovery time upon washout to a single exponential.

This time constant was comparable to that measured for O-O patches. **Panel E** shows the mean association time constant for 4.0 μM GsMTx4 as $\tau_a = 10.4 \pm 3.0$ s (SD). The rate constant, τ_d, gave a dissociation rate of k_d=0.10 s$^{1.}$ However, τ_a was dominated by k_d, and, unlike the rate constant from outside-out patches, the equilibrium constant calculation was untrustworthy.